Analyzing the Relationship Between Spatial Distribution of Air Pollutant Concentrations and Land Cover Over Iran

Saeedeh Nasehi[1]✉ | Ahmad Nohegar[2]

1. Department Landscape Artitecture, Minab Higher Education Center, University of Hormozgan, Bandar Abbass, Iran
2. Graduate Faculty of Environment, University of Tehran, P.O.Box 14155-6135, Tehran, Iran

Article Info	ABSTRACT
	Air pollution is a major environmental challenge, exacerbated by urban and industrial expansion, with significant impacts on human health and climate change. This study, using advanced remote sensing technology and Sentinel-5 satellite data, examines the relationship between seven land cover types and air pollutants in Iran for the years 2022 and 2023. Pearson correlation analysis was applied to assess these relationships. Standardized pollutant concentration maps were generated using combination operators such as "AND," "OR," "SUM," and "GAMMA 0.5" within Arc Map software to identify high-risk pollution areas. The results indicated that Tehran, Karaj, and Isfahan had the highest nitrogen dioxide concentrations, while Ahvaz, Bandar Abbas, Bushehr, and Arak recorded the highest sulfur dioxide levels. Aerosol concentrations were highest in Zahedan, Yazd, and Qom, while Tehran, Bandar Abbas, and Ahvaz showed elevated carbon monoxide levels. Northern cities like Ardabil, Urmia, and Rasht had the highest ozone concentrations. Findings revealed a negative correlation between tree density and aerosol levels, and a positive correlation between barren lands and aerosols. There was also a direct correlation between industrial and built-up areas and pollutants such as sulfur dioxide, carbon monoxide, and nitrogen dioxide. However, no specific relationship was found between ozone concentrations and land cover types, suggesting that ozone levels are more geographically influenced. The combined maps highlighted Tehran and industrial cities as high-risk areas for air pollution, emphasizing the importance of increasing dense vegetation and proper land use management as effective strategies for mitigating air pollution.

INTRODUCTION

In today's world, air pollution has emerged as one of the most critical environmental challenges, particularly impacting human life quality, especially in developing countries (Kazemi Garajeh et al., 2023). With the rapid pace of urbanization, it is projected that by 2050, over half of the global population will reside in urban areas (UNDESA, 2018; Sun et al., 2020; Wang et al., 2021; Nasehi et al., 2023). This urban growth has driven significant changes in land use and cover, along with a sharp increase in energy consumption (Wang et al., 2021; Zheng et al., 2017). Urban areas, as the primary hubs of population density, experience the most substantial shifts in land use, resulting in higher emissions of air pollutants (Huang et al., 2021). Air pollutants alter urban atmospheric conditions through complex physical and chemical processes, leading to issues such as acid rain, ozone layer depletion, damage to ecosystems and agricultural crops, as well as economic and aesthetic impacts (Zhu et al., 2019; Wang et al., 2021). These pollutants originate from various sources, including industries, urban traffic,

and fossil fuel combustion, each posing distinct threats to human health and the environment (Ghannadi et al., 2022; Zabalza et al., 2007; Flemming et al., 2005).

For instance, sulfur dioxide (SO_2) primarily originates from power plants, heavy industries, and urban traffic, and its levels are rising due to increased energy consumption and economic growth (Castelhano, 2019; Fuladlu & Altan, 2021). Carbon monoxide (CO) is produced through the incomplete combustion of carbon-containing fuels, with its main sources being industrial processes and motor vehicles (Brunelli et al., 2007; El-Fadel & Abi-Esber, 2009). Nitrogen dioxide (NO_2) is generated from the combustion of fossil and biomass fuels, while ozone concentrations tend to peak in the summer as another significant pollutant (Krotkov et al., 2016; Xue et al., 2020; Gharibi & Shayesteh, 2021). Additionally, particulate matter enters the atmosphere from both natural sources, such as dust storms, and human activities, including transportation and industrial operations (Ghannadi et al., 2022; Nasehi et al., 2023).

Monitoring and measuring these pollutants is essential for managing and controlling critical environmental conditions. Although air quality monitoring stations provide some of the most accurate measurements, their coverage is limited to nearby areas, and their high costs restrict widespread application (Filonchyk et al., 2018). In this context, high-resolution remote sensing emerges as a viable alternative. Sentinel satellites, including Sentinel-5, are equipped to detect and monitor pollutants such as ozone, methane, aerosols, sulfur dioxide, nitrogen dioxide, and carbon monoxide. They offer valuable data for environmental management and the monitoring of climate change and air pollution (Kazemi Garajeh et al., 2023; Lin et al., 2022; Naboureh et al., 2021).

Research has demonstrated that land cover significantly impacts air quality. For instance, Zhu et al. (2019) found a positive correlation between the concentration of pollutants such as ozone, carbon monoxide, and sulfur dioxide and the expansion of agricultural land in China. Conversely, an increase in forested areas was associated with a decrease in these pollutants. Other studies have also indicated that regions characterized by low vegetation and high urban development density typically exhibit elevated concentrations of pollutants (Weng & Yang, 2006; Zheng et al., 2017; Gheshlaghpoor et al., 2023).

The primary objective of this research is to develop and present an innovative approach for analyzing the spatial distribution of air pollutant concentrations in relation to land cover on a macro scale in Iran. To achieve this, the study employs a novel combination of advanced remote sensing technologies utilizing Sentinel-5 satellite data, statistical analyses, and Geographic Information Systems (GIS). This research uniquely utilizes composite operators within the ArcMap environment and the Python API to generate standardized maps of pollutant concentrations and identify areas at high risk of air pollution. Additionally, the precise categorization of land cover into seven classes, along with a comprehensive examination of the effects of each land cover type on pollutant concentrations, represents another innovative aspect of this study. This comprehensive approach facilitates a more accurate assessment of the spatial distribution of air pollution at a macro scale.

MATERIALS AND METHODS

The area of study is Iran, a country situated in West Asia and at the heart of the Middle East. It covers an approximate area of 1.64 million square kilometers and is positioned between latitudes 25 to 40 degrees north and longitudes 44 to 64 degrees east (Figure 1).

In this study, satellite images from the Level 3 TROPOMI sensor aboard the Sentinel-5 satellite, with a spatial resolution of 1,000 by 1,000 meters, were used to assess air pollutant concentrations during the period from January 1, 2022, to December 30, 2023. For each pollutant, a specific set of bands was utilized as outlined in Table 1. To accomplish this, JavaScript coding was employed in the Google Earth Engine environment to extract the average concentration of
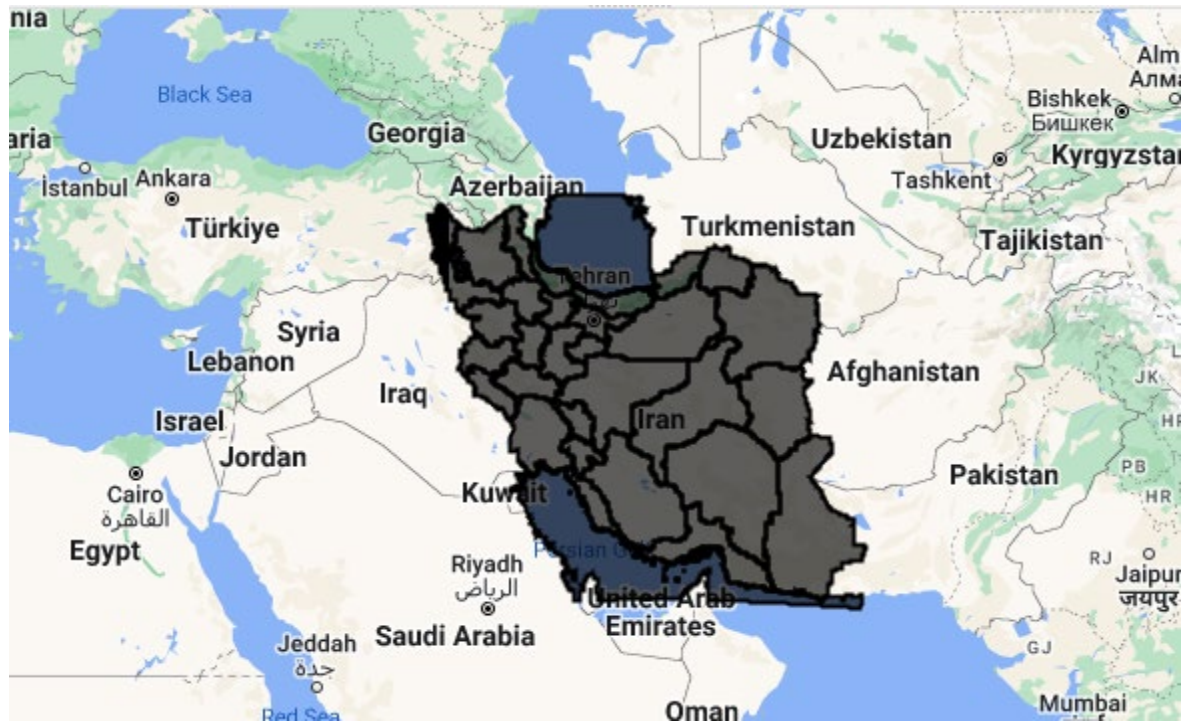
Fig. 1. study area

Table 1. Sentinel-5 Product Specifications for Analyzed Pollutants

Pollutant Name	Product	Dataset	Description/Unit/Band
Carbon Monoxide	Sentinel - 5P NRTI CO: Near Real -Time Carbon Monoxide	COPERNICUS /S5P/NRTI/L3 _CO	CO_column_number_density/ mol/m² / Vertically integrated CO column density.
Aerosol	Sentinel - 5P NRTI AER AI: Near Real -Time UV Aerosol Index	COPERNICUS /S5P/NRTI/L3 _AER_AI	absorbing_aerosol_index/ - / A measure of the prevalence of aerosols in the atmosphere, calculated by this equation using the 354 /388 wavelength pair.
Nitrogen Dioxide	Sentinel - 5P NRTI NO_2: Near Real -Time Nitrogen Dioxide	COPERNICUS /S5P/NRTI/L3 _NO_2	NO_2_column_number_density/ mol/m² / Total vertical column of NO_2 (ratio of the slant column density of NO_2 and the total air mass factor)
Ozone	Sentinel - 5P NRTI O_3: Near Real -Time Ozone	COPERNICUS /S5P/NRTI/L3 _O_3	O_3_column_number_density/ mol/m² / Total atmospheric column of O_3 between the surface and the top of atmosphere, calculated with the DOAS algorithm
Sulphur Dioxide	Sentinel - 5P NRTI SO_2: Near Real – Time Sulphur Dioxide	COPERNICUS /S5P/NRTI/L3 _SO_2	SO_2_column_number_density/ mol/m² / SO_2 vertical column density, calculated using the DOAS technique.

air pollution data for the area under investigation.

Subsequently, the final map of average pollutant concentrations was transferred to Arc Map for analysis. In this stage, statistical data related to the average concentrations of pollutants were processed and analyzed using SPSS. To examine the spatial distribution of each pollutant

in relation to land cover, a land cover map for 2022 was generated using satellite imagery from Google Earth Engine. The classification of land cover was based on the Stewart and Oke model and was divided into eight categories: built-up areas, rocky industries, dense tree cover, scattered trees, shrub land, scrubland, sparse vegetation, and bare soil or sand (Table 2). After creating this map, it was converted into vector layers to facilitate more detailed analyses, and a land cover density map was developed in Arc Map.

Next, the spatial distribution of each pollutant was analyzed in relation to land cover density using regression analysis. This analysis was based on 6,606 sampling points, allowing for a more precise understanding of the relationship between pollutants and land cover. To generate a comprehensive map of total pollutant concentrations, the spatial distribution maps for each pollutant were standardized to a scale of zero to one. Subsequently, these standardized data were combined in Arc Map using fuzzy operators such as AND, OR, SUM, PRODUCT, and GAMMA 0.5. Each of these operators was specifically designed to identify areas with varying pollution risk levels. These combined methods are particularly effective for pinpointing regions at high risk of pollution, providing policymakers with accurate scientific data to make more informed decisions regarding air quality management and pollution reduction strategies.
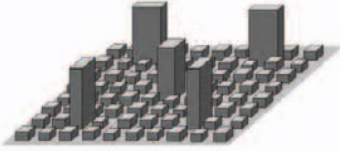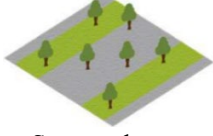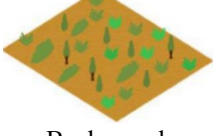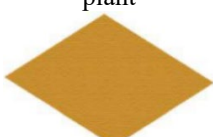
RESULTS AND DISCUSSION
Spatial distribution of pollutants concentration

Figure 2 illustrates the spatial distribution of the concentration of main air pollutants in Iran for 2022 and 2023: AI, NO_2, SO_2, CO and O_3. In terms of NO_2 pollution, Tehran (0.000692), Karaj (0.000405), Isfahan (0.000266), Mashhad (0.000247), Qom (0.000191), Shiraz (0.000184), Tabriz (0.000181) and Rasht (0.000173) mol/m^2 respectively have the highest values. They are big cities with heavy traffic on the main roads that have increased the concentration of this pollutant. The cities of Zahedan (1.061896), Yazd (0.86996), Qom (0.747929), Birjand (0.738589), Bushehr (0.7179) and Bandar-Abbas (0.71568) have the highest absorbing aerosol index. The highest concentration of aerosols is in the southern, eastern, and central regions of Iran. Conversely, the northern cities of Iran have the lowest concentration of this pollutant due to dense vegetation. The cities of Tehran (0.036146), Bandar-Abbas (0.034399), Rasht (0.034325), Ahvaz (0.033867) and Bushehr (0.032976) mol/m^2 respectively have the highest average concentration of CO pollutants. The concentration of this pollutant is higher in densely populated cities with heavy traffic and industrial areas. The cities of Ardabil (0.137973), Urmia (0.137964), Rasht (0.137851), Tabriz (0.13761) and Gorgan (0.135844) mol/m^2 also have the highest amount of ozone pollutants. In general, the northern regions of the country have higher concentrations of ozone pollutants, while the southern regions of the country have lower concentrations of this pollutant.

Land cover classes

Land cover classes were classified into 8 classes including Built-up areas, Heavy industries, dense trees, scattered trees, Bush, scrub, Low plant, bare soil or sand and water in Iran. In addition Figure 3 illustrates that dense trees cover an area of 33,719.30 square kilometers. This type of cover is predominantly found in the northern and northwestern regions of the country. Additionally, scattered trees covering 176,811.15 square kilometers are present in various parts of the country, particularly in the mountainous and semi-mountainous regions of the western areas. Also, bush, scrub are found in different regions of the country, especially in arid and semi-arid areas. This type of land cover plays an important role in preserving soil and preventing desertification, covering an area of 815,265.19 square kilometers. Herbaceous plants or crops /Low plant span an area of 264,280.48 square kilometers. Barren lands, covering 321,949.73 square kilometers, are also prevalent in arid and semi-arid regions. Most of these lands - are located in the central plateau of the country. Lastly, built-up lands occupy an area of

Table 2. Description of land cover classes (stewart & oke, 2012)

Explanation	Land cover classes
Urban and rural built-up areas	Built-up areas
Industrial zones	Heavy industries
Heavily wooded landscape of deciduous and/or evergreen trees. Land cover mostly pervious (low plants). Zone function is natural forest, tree cultivation, or urban park.	Dense trees
Lightly wooded landscape of deciduous and/or evergreen trees. Land cover mostly pervious (low plants). Zone function is natural forest, tree cultivation, or urban park.	Scattered trees
Open arrangement of bushes, shrubs, and short, woody trees. Land cover mostly pervious (bare soil or sand). Zone function is natural scrubland or agriculture.	Bush, scrub
Featureless landscape of grass or herbaceous plants/crops. Few or no trees. Zone function is natural grassland, agriculture, or urban park.	Herbaceous plants or crops /Low plant
Featureless landscape of soil or sand cover. Few or no trees or plants. Zone function is natural desert or agriculture.	Bare soil or sand
Large, open body of water such as seas and lakes	water

9,506.80 square kilometers. These lands include both urban and rural areas, accounting for a small percentage of the country's total land area.

Spatial assessment of Land cover density

Figure 4 displays the spatial distribution map of land cover density. The density map of industries in Figure 4 is prepared using statistical data related to the number of industrial units.
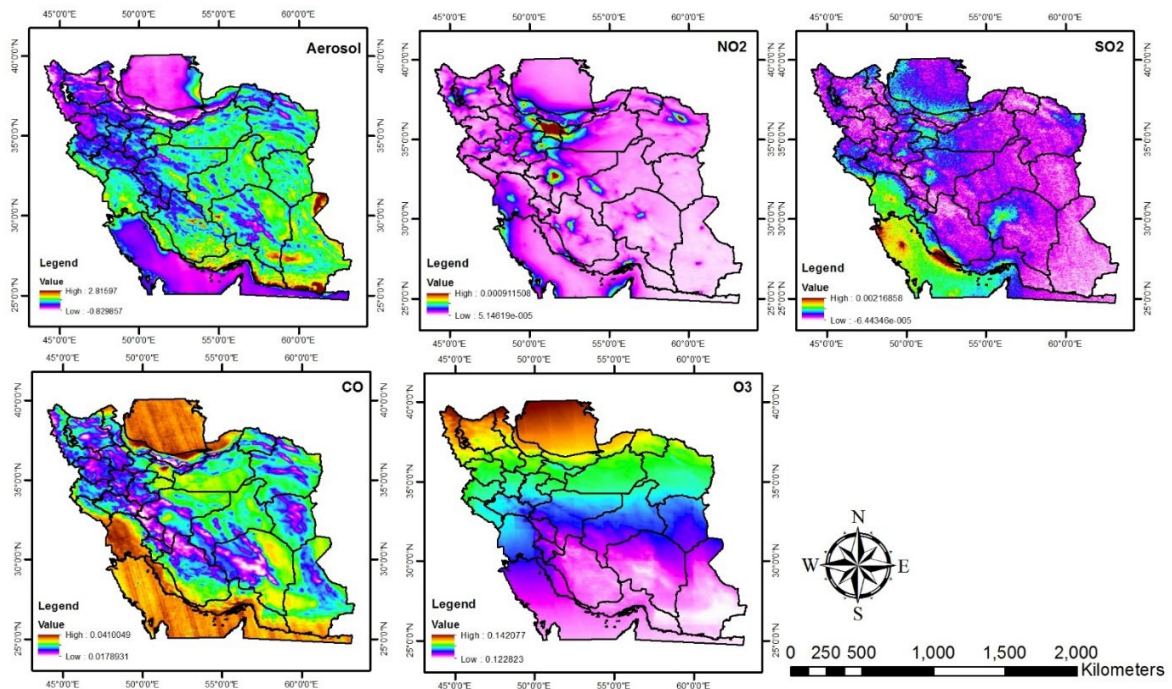
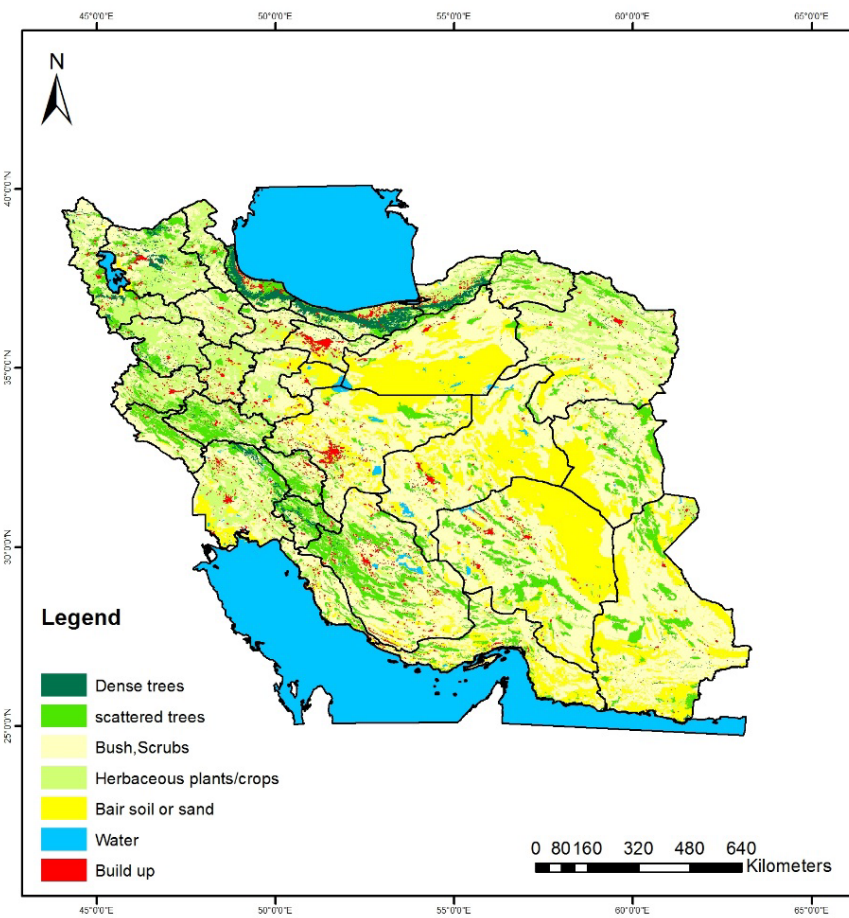**Fig. 2.** Spatial distribution of pollutant concentration over Iran in 2022 and 2023

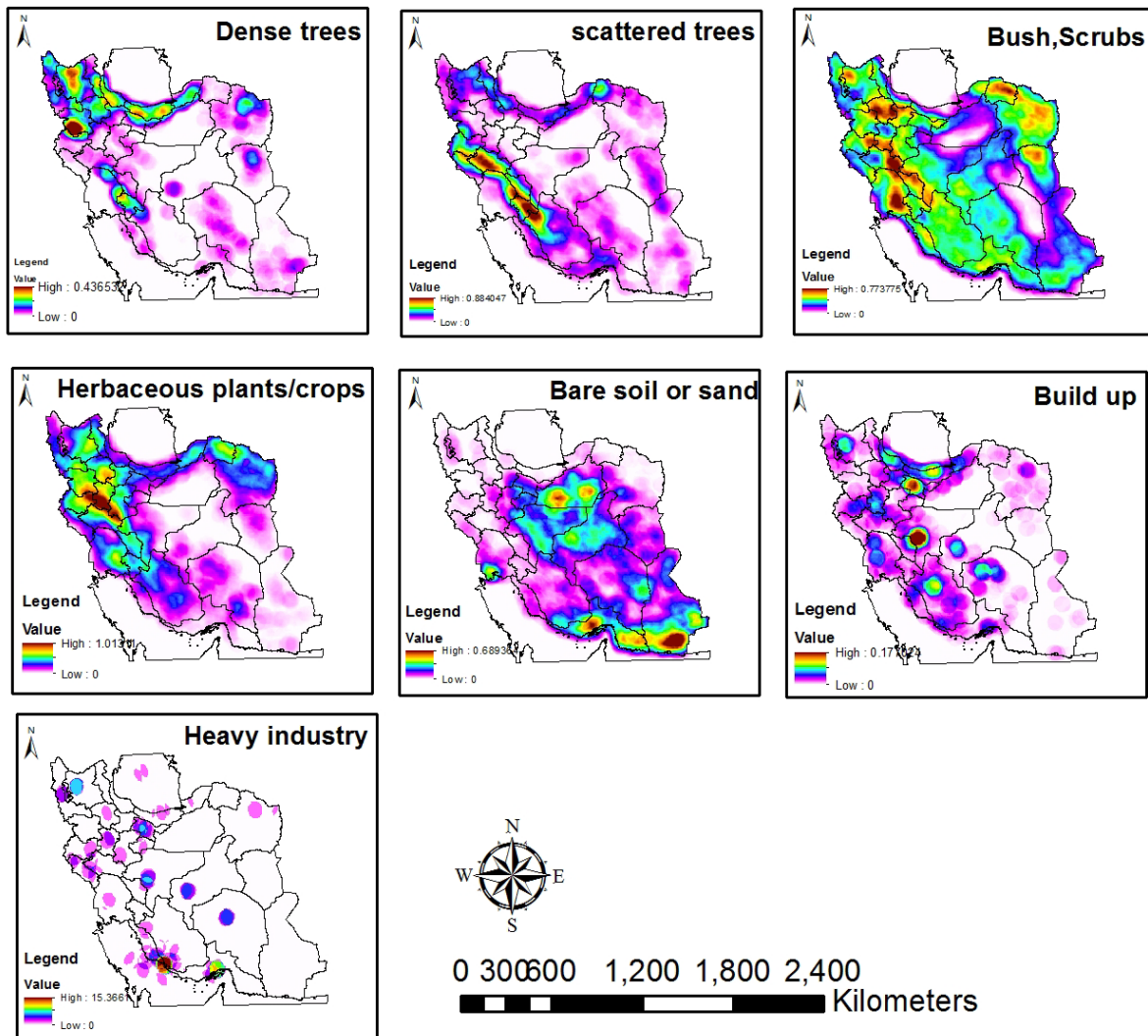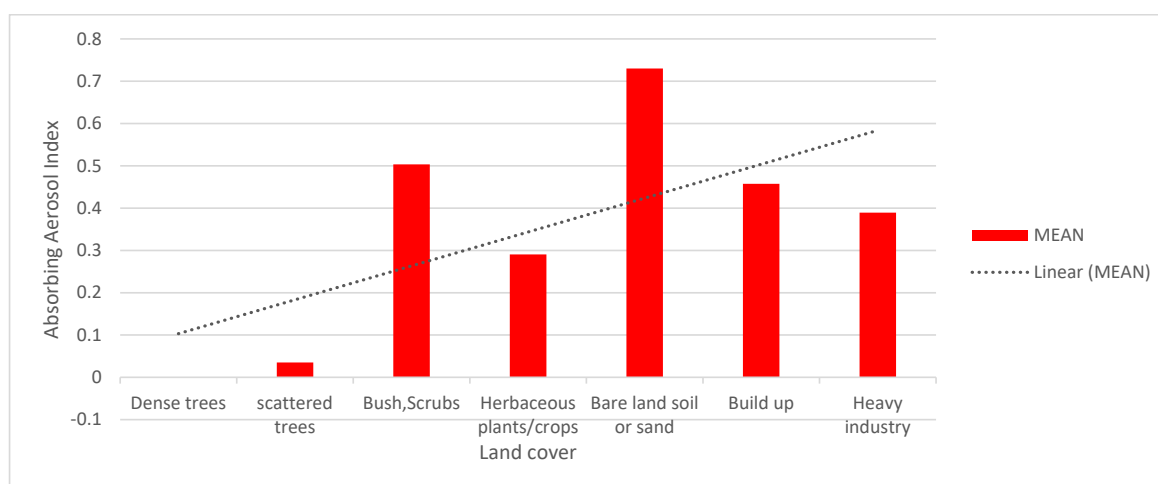**Fig. 3.** Land cover classes in Iran

Fig. 4. Land cover density maps

Notably, cities such as Tehran, Ahvaz, Bushehr, Bandar Abbas, Arak, Isfahan, and Tabriz exhibit a high density of industrial units.

Relationship between the type of land cover and the concentration of air pollutants

The aerosol absorption index, derived from Sentinel-5 satellite imagery using Google Earth Engine, reveals a clear link between land cover types and aerosol absorption levels in the atmosphere) Figure 5(. The index generally records its lowest values in areas with vegetation, such as dense trees (-0.001), shrubs (0.03518), and low plant (0.29). In forested regions, the negative value of the index indicates cleaner air, with fewer light-absorbing particles. This suggests that there is little to no absorption of light by suspended particles in these areas.

In contrast, the index reaches its highest value (0.73) in sparsely vegetated areas, such as bare land, indicating higher levels of light absorption by aerosols and consequently, greater air pollution. Urbanized areas, with an average index of 0.457349, and heavy industrial zones, averaging 0.389364, also significantly contribute to elevated aerosol levels, primarily due to construction and industrial activities that release particulate matter directly into the environment.

Vegetation, particularly trees and shrubs, helps lower the aerosol absorption index in

Fig. 5. Aerosol over different land cover classes over Iran in 2022 and 2023
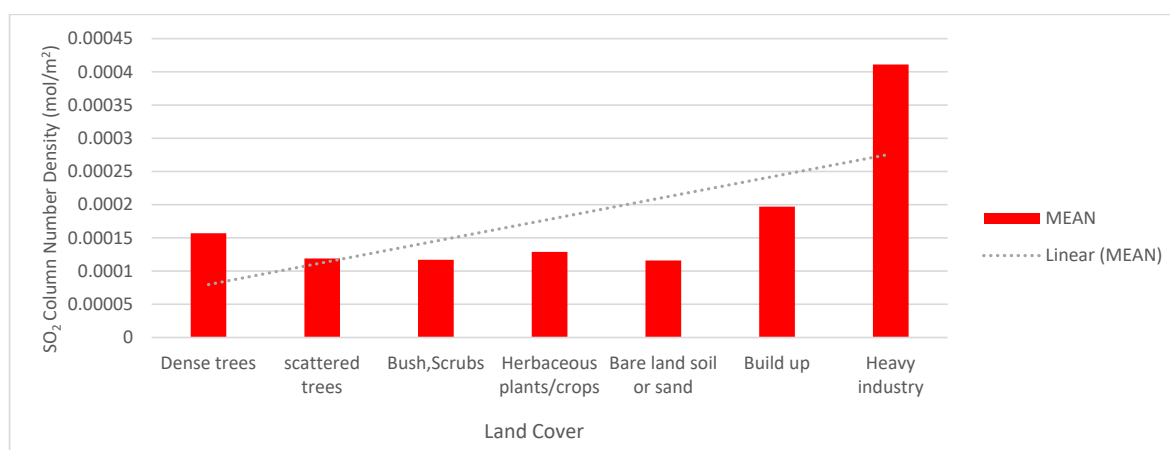
Fig. 6. SO_2 over different land cover classes over Iran in 2022 and 2023

surrounding areas by capturing airborne particles, aligning with the findings of Nowak et al. (2006) on the role of vegetation in particulate matter removal. Conversely, barren lands act as major sources of aerosol pollution.

An analysis of the relationship between sulfur dioxide concentrations and land cover types, based on average values, reveals that different land covers have distinct impacts on SO_2 levels (Figure 6). Heavy industrial areas exhibit the highest SO_2 concentrations, with an average of 0.000411 mol/m². This elevated concentration indicates significant pollution sources, which can have serious consequences for air quality and environmental health.

Carmichael et al. (2002) emphasize that industrial facilities, particularly those burning fossil fuels such as coal and oil for energy production, are among the primary contributors to SO_2 emissions. This correlation highlights the critical role of industrial activities in the release of this pollutant. Built-up areas, with an average SO_2 concentration of 0.000197 mol/m², rank next in terms of emissions. These areas are significant SO_2 sources due to traffic, construction activities, and local factories. The elevated SO_2 levels in these regions underscore the necessity of implementing control measures in urban planning and resource management.

In contrast, vegetated areas, such as dense trees (with an average SO_2 concentration of 0.000157 mol/m²) and scattered trees (0.000119 mol/m²), function as natural filters that can
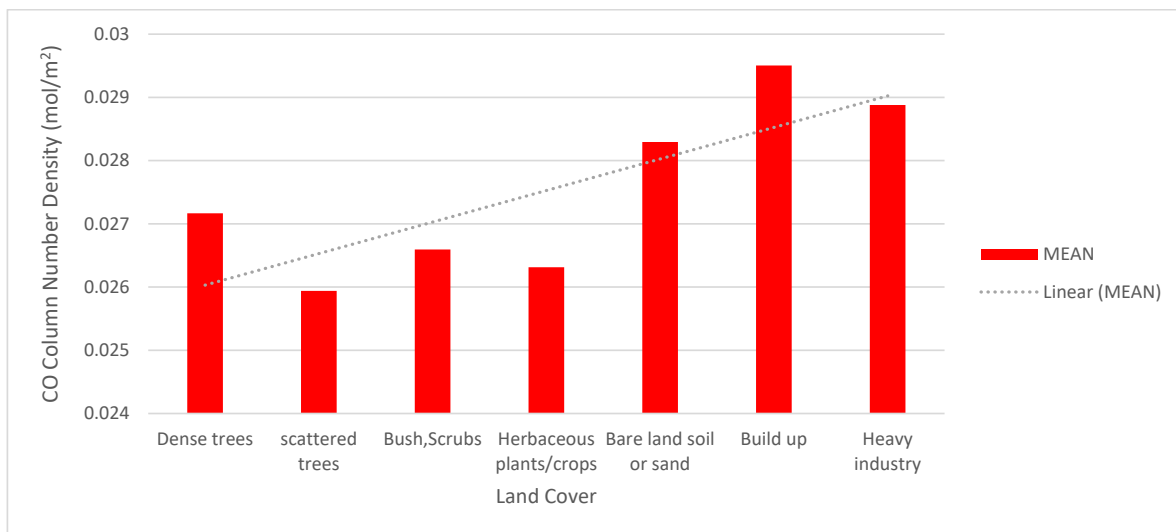
Fig. 7. CO over different land cover classes over Iran in 2022 and 2023

absorb a portion of pollutants. Research has shown that these types of vegetation play an important role in reducing SO_2 concentrations.

However, brush and scrubs (with an average SO_2 concentration of 0.000117 mol/m²) and herbaceous plants or agricultural crops (0.000129 mol/m²) still experience pollution, and their absorption capacity is more limited. This suggests that simply having vegetation is insufficient; the type and density of plant cover are also critical factors to consider.

Bare land and exposed soil, with an average SO_2 concentration of 0.000116 mol/m², lack the ability to absorb SO_2 due to the absence of vegetation and may serve as sources of dust and other pollutants. The absence of vegetation in these areas leads to the loss of natural pollutant absorption capacities, which can exacerbate air quality issues.

In conclusion, heavy industrial and urban areas have the most significant impact on increasing sulfur dioxide concentrations, emphasizing the need for strategies to expand vegetation cover and green spaces in these regions to reduce pollution and improve air quality. These findings clearly demonstrate that land cover types, particularly in relation to sulfur dioxide, play a key role in air pollution management, and enhancing vegetation cover can be an effective strategy for mitigating pollutants.

Figure 7 illustrates the relationship between CO concentrations and various land cover types, highlighting that different land covers exert distinct influences on CO levels.According to the data, build up area and heavy industry exhibit the highest average CO concentrations, at 0.029504 and 0.028879 mol/m², respectively. This suggests that urban and industrial areas, due to human activities such as traffic, industrial production, and fossil fuel consumption, are the primary sources of CO emissions. Zhang et al. (2017) also found a positive correlation between building density and CO pollutants.

Bare land and exposed soil, with an average CO concentration of 0.028294 mol/m², indicate that these areas can also contribute to increased CO levels, as the lack of vegetation can create unfavorable conditions for air quality.

In contrast, vegetated areas, such as dense and scattered trees, as well as shrubs and herbaceous plants, naturally have lower CO concentrations compared to other land cover types, demonstrating their ability to absorb and reduce pollutant levels. For instance, dense and scattered trees, with average CO concentrations of 0.027166 and 0.025939 mol/m², respectively, can serve as positive elements for improving air quality. Zhu et al. (2019) similarly confirm the negative relationship between forest cover and dense trees with CO concentrations.
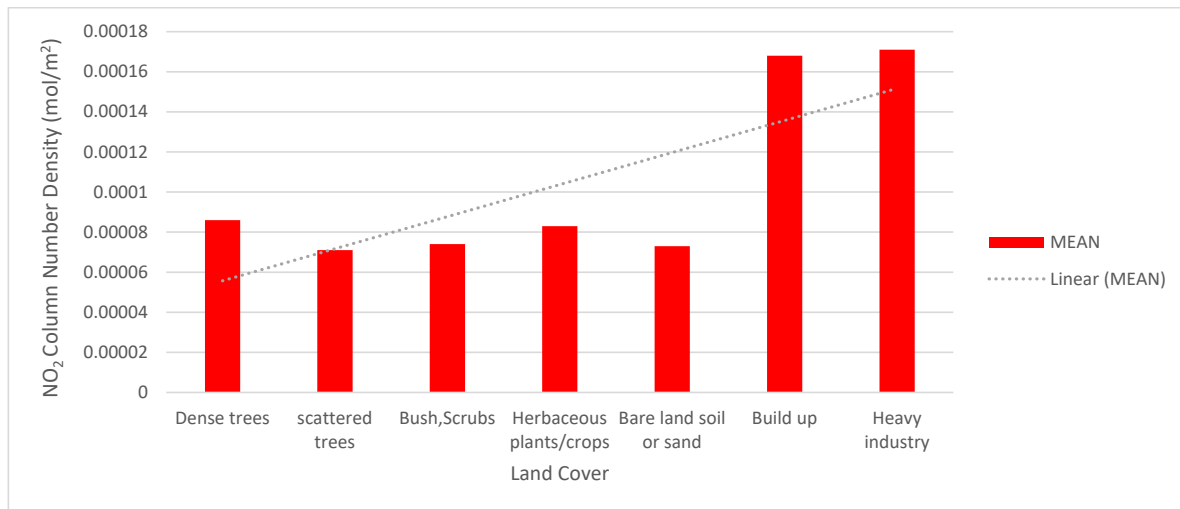
Fig. 8. NO$_2$ over different land cover classes over Iran in 2022 and 2023
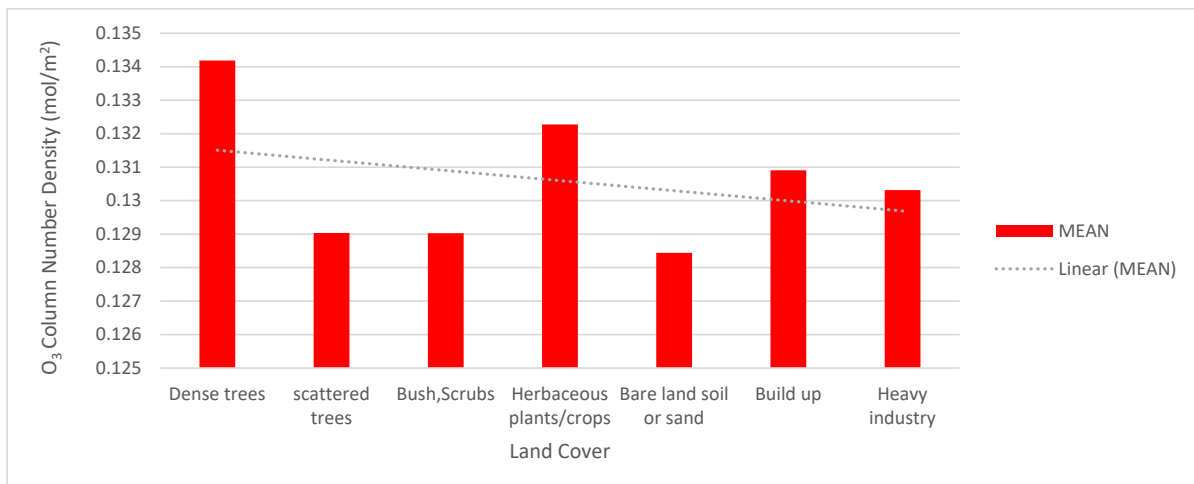

Fig. 9. O3 over different land cover classes over Iran in 2022 and 2023

These findings suggest that the presence of dense vegetation in urban areas can significantly reduce CO concentrations. Therefore, proper environmental planning and management to increase green spaces and vegetation cover is essential. This highlights the need for policies and strategies aimed at protecting and expanding these natural resources to mitigate pollution and enhance air quality.

According to Figure 8, heavy industry and built-up areas exhibit the highest NO$_2$ concentrations, with averages of 0.000171 μg/m³ and 0.000168 μg/m³, respectively. This indicates the significant impact of industrial activities and urban development on increasing NO$_2$ levels. Activities such as the burning of fossil fuels in industries and heavy traffic in urban areas are identified as the primary sources of NO$_2$ emissions.

In comparison to natural land covers, dense trees and scattered trees show lower NO$_2$ concentrations, with averages of 0.000086 μg/m³ and 0.000071 μg/m³, respectively. This suggests that vegetation can help absorb and reduce pollutants, playing an important role in improving air quality. These results are consistent with the findings of Rodríguez et al. (2016), King et al. (2014), and McCarty & Kaza (2015).

According to Figure 9, the O$_3$ pollutant does not appear to have a significant correlation with

Table 3. The relationship between air pollutants with land cover

Landcovers \ Pollutants	Dense trees	Scattered trees	Brush, Scrubs	Herbaceous plants/Crops	Bare land soil or sand	Build up	Heavy industry
AI	-.351[*]	-.091[*]	.116[*]	-.220[*]	.556[*]	.104[*]	.031[*]
SO_2	-.135[*]	-.117[*]	-.281[*]	-.157[*]	-.227[*]	.113[*]	.392[*]
CO	-.333[*]	-.322[*]	-.559[*]	-.074[*]	-.038[*]	.039[*]	.009[*]
NO_2	-.165[*]	-.041[*]	.058[*]	.122[*]	.379[*]	.534[*]	.326[*]
O_3	.228[*]	-.029[*]	-.065[*]	-.003[*]	-.087[*]	-.017[*]	-.018[*]

[*]. Correlation is significant at the 0.01 level (2-tailed).

different land cover types on a macro scale. However, the northern regions of the country show higher concentrations compared to the southern regions. Huang et al. (2017) confirm that the annual average ozone levels vary depending on geographical longitude and terrain conditions, and are mainly influenced by regional factors.

Table 3 illustrates the relationship between land cover types and air pollutants. Each cell in this table displays the correlation coefficient between the density of a specific land cover type and the concentration of a particular pollutant. The numerical correlation coefficient ranges from -1 to 1. A positive correlation coefficient indicates that the pollutant concentration increases with higher land cover density, while a negative correlation coefficient signifies that the pollutant concentration decreases as land cover density increases.

The density of all land cover types, except barren lands, built up area, industrial areas, Brush and Scrubs, exhibits a negative relationship with the concentration of aerosols. In other words, as vegetation and trees increase, the aerosol concentration decreases. Additionally, dense trees are negatively correlated with aerosol concentration, indicating their effective role in absorbing aerosols and purifying the air. Interestingly, there is a positive relationship between barren lands and bare lands and the concentration of aerosols. The density of all land cover types, except built up area and industrial areas, shows a negative relationship with the concentration of sulfur dioxide. However, there is a positive correlation between this pollutant's concentration and industrial areas. This research demonstrates a positive relationship between this pollutants and built up areas, while other land cover types exhibit a negative relationship. In other words, as urban development increases, so does the concentration of carbon monoxide. Conversely, areas with different land covers show lower CO concentrations. The density of all land cover types, except barren lands, built up areas, industrial zones, scrubland and cultivated/agricultural lands (low plant area), negatively correlates with nitrogen dioxide concentration. Notably, built up areas exhibit a strong positive correlation with NO_2 pollution. Additionally, the positive relationship between agricultural and crop lands and NO_2 pollutant is attributed to pesticide and fertilizer use (Almaraz et al., 2018; Berihun et al., 2019). Interestingly, there is no specific relationship between land cover and ozone pollutant concentration. Zhang et al. (2017) concluded that the correlation between land use and ozone pollution is weak (Zheng et al., 2017).

Analysis of distribution maps of air pollutants using operators

In the figure 10, the map of Iran is displayed, with each corresponding to an operator in Arc Map. These operators include AND, OR, SUM, PRODUCT, and GAMMA (with a factor of 0.5). Each of these maps is derived from the combination of five pollutant maps: CO, SO_2, NO_2, AI, and O_3, all standardized within the range of 0 to 1.

AND map displays the ranges where all five pollutants are present simultaneously. In other words, these areas have the highest cumulative concentration of pollutants. OR map shows the ranges where at least one of the five pollutants is present. In other words, these areas have
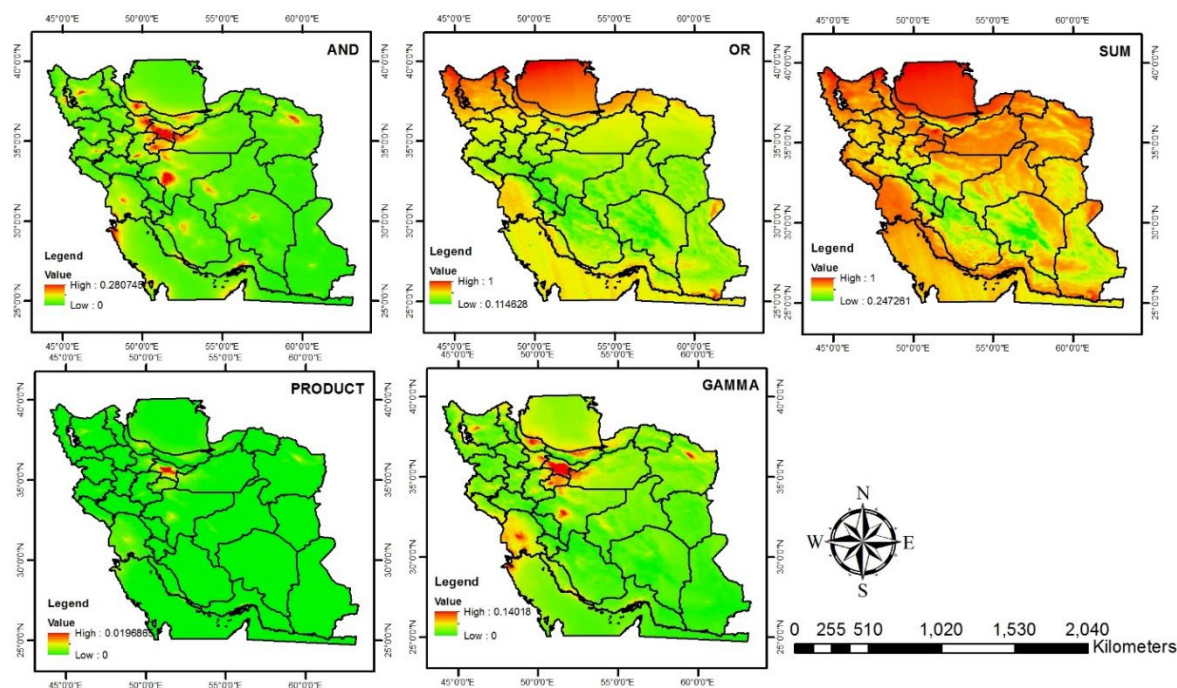
Fig. 10. Distribution maps of air pollutants using AND, OR, SUM, PRODUCT, and GAMMA 0.5 operators

moderate levels of pollutant concentrations.

SUM map illustrates the total values of all five pollutants at each location. It can be used to identify areas with the highest levels of air pollution. Essentially, this map represents the overall concentration of pollutants in each area and indicates the pollutant amount in those regions.

PRODUCT map displays the product of the values of all five pollutants at each location. It can be used to identify areas at risk of cumulative effects from pollutants. In other words, this map shows how pollutants interact with each other, potentially having harmful effects on human health and the environment. GAMMA0.5 map shows the square root of the product of the values of all five pollutants at each location. It can be used to identify areas at risk of nonlinear effects from pollutants. The presented maps reveal significant differences in pollutant concentrations across various regions of Iran. Metropolises and industrial centers exhibit the highest pollutant levels, while areas with vegetation and rural landscapes have lower concentrations. Notably, Tehran, as a major metropolis, consistently displays high pollution levels in all composite maps, making it a critical focal point for air quality management in Iran.

The findings of this research indicate that land cover plays a crucial role in determining air quality. Based on these results, more effective and targeted management programs can be developed to reduce air pollution in Iran. Such programs should be tailored to the specific conditions of each region, taking into account various factors, including land cover types, industrial activities, and climatic conditions.

The results demonstrate that an increase in dense tree cover and forested areas significantly enhances air quality, whereas industrial development and urban expansion exacerbate air pollution. For sustainable urban development, greater emphasis must be placed on forest conservation, and urban planning should be conducted in a way that maintains a balance among different land uses. Based on this research, industrial cities and large urban areas are among the regions with the highest air pollution risk. Metropolitan areas like Tehran, Karaj, and Isfahan, due to heavy traffic and industrial activities, exhibit the highest concentrations of nitrogen

dioxide. Industrial and refinery hubs such as Ahvaz, Bandar Abbas, and Bushehr experience elevated levels of sulfur dioxide due to their extensive industrial operations. Southern, eastern, and central regions of Iran face high concentrations of Aerosol, especially due to dust storms and industrial activities, with cities like Zahedan, Yazd, and Qom being particularly affected. Large cities and industrial centers such as Tehran, Bandar Abbas, and Rasht show high levels of carbon monoxide because of heavy traffic and industrial emissions. Interestingly, northern regions of the country display higher ozone levels, likely due to their unique geographical conditions. To improve air quality in Iran, the following actions are essential: re-purposing contaminated land for lower-risk uses, creating green belts, and increasing vegetation in urban and industrial areas. Implementing stricter standards for industries, advancing pollution control technologies, and preventing the destruction of forests and grasslands are also critical. Restoration of degraded areas and tree planting in urban and industrial zones should be prioritized, alongside reducing traffic in major cities by expanding public transportation. Strict monitoring of polluting industries, enforcing stringent environmental regulations, promoting clean technologies, and developing low-carbon industries are necessary steps. Additionally, measures to combat dust storms, such as stabilizing moving sand dunes, increasing urban and industrial green cover, establishing a comprehensive network of air quality monitoring stations, and raising public awareness about the importance of air quality are crucial. By implementing these strategies and fostering interdepartmental collaboration, significant improvements in air quality and public health can be achieved. Furthermore, conducting additional research on the impacts of climate change on air pollution, along with the development of more accurate pollution forecasting models, will support the creation of more comprehensive and effective action plans.

CONCLUTION

Air pollutant concentrations are measured by ground-based monitoring stations with high accuracy but limited to specific points. Due to the restricted coverage of these stations, estimating pollutant levels over larger distances is not feasible. The spatial distribution of pollutants, as observed through remote sensing imagery, indicates that to effectively identify polluted areas on a macro scale, continuous satellite data that measure atmospheric pollutants daily must be utilized. In this study, air pollution in Iran was monitored using Sentinel-5 satellite imagery and the Google Earth Engine platform over the years 2022 and 2023. The findings revealed a negative correlation between tree density and aerosol concentrations, while a positive correlation was observed between barren land areas and aerosol levels. A direct relationship was also identified between the density of industrial and built-up areas and the concentrations of pollutants such as SO_2, CO, and NO_2. No significant correlation was found between O_3 levels and land cover types, suggesting that ozone concentration is more influenced by geographical factors. The analysis of different operator maps highlighted significant variations in pollutant concentrations across Iran, with the highest levels concentrated in major cities and industrial zones. Tehran emerged as one of the most critical hotspots for air pollution. To enhance air quality monitoring, it is recommended to strengthen monitoring networks in key areas and utilize satellite data to identify the need for new stations. Policymakers should implement pollution reduction measures, such as planting vegetation and enforcing stricter regulations, particularly in highly industrialized and polluted regions. Supporting greening initiatives and expanding urban green spaces is also essential. The development of air quality forecasting models and long-term research is advised for more effective pollution management. Future studies should incorporate additional parameters, such as Digital Elevation Models (DEM), wind patterns, and population data, to inform better planning and policy decisions.

GRANT SUPPORT DETAILS

CONFLICT OF INTEREST

The authors declare that there is not any conflict of interests regarding the publication of this manuscript. In addition, the ethical issues, including plagiarism, informed consent, misconduct, data fabrication and/ or falsification, double publication and/or submission, and redundancy has been completely observed by the authors.

LIFE SCIENCE REPORTING

No life science threat was practiced in this research.

REFERENCES

Almaraz, M., Bai, E., Wang, C., Trousdell, J., Conley, S., Faloona, I., & Houlton, B. Z. (2018). Agriculture is a major source of NOx pollution in California. Sci. Adv., 4(1), eaao3477.

Berihun, , M. L., Tsunekawa, A., Haregeweyn, N., Meshesha, D. T., Adgo, E., Tsubo, M., Masunaga, T., Fenta, A. A., Sultan, D., & Yibeltal, M. (2019). Exploring land use/land cover changes, drivers and their implications in contrasting agro-ecological environments of Ethiopia. Land Use Policy, 87, 104052.

Brunelli, U., Piazza, V., Pignato, L., Sorbello, F., & Vitabile, S. (2007). Two-days ahead prediction of daily maximum concentrations of SO_2, O_3, PM_{10}, NO_2, CO in the urban area of Palermo, Italy. Atmos. Environ., 41(4), 2967-2995.

Carmichael, G. R., Streets, D. G., Calori, G., Amann, M., Jacobson, M. Z., Hansen, J., & Ueda, H. (2002). Changing trends in sulfur emissions in Asia: implications for acid deposition, air pollution, and climate. Environ. Sci. Technol., 36(22), 4707-4713.

Castelhano, F. J. (2019). Sulfur dioxide: Behaviour and trends at the industrial city of Araucaria/Brazil. J. Air Pollut. Health, 4(4), 227-240.

El-Fadel, M., & Abi-Esber, L. (2009). In-vehicle exposure to carbon monoxide emissions from vehicular exhaust: A critical review. Crit. Rev. Environ. Sci. Technol., 39(8), 585-621.

Epa, U. (2016). Particulate matter (PM) basics. USA: United States Environmental Protection Agency.]

Filonchyk, M., Yan, H., Yang, S., & Lu, X. (2018). Detection of aerosol pollution sources during sandstorms in Northwestern China using remote sensed and model simulated data. Adv. Space Res., 61(4), 1035-1046.

Flemming, J., Stern, R., & Yamartino, R. (2005). A new air quality regime classification scheme for O_3, NO_2, SO_2 and PM_{10} observations sites. Atmos. Environ., 39(33), 6121-6129.

Ghannadi, M. A., Shahri, M., & Moradi, A. (2022). Air pollution monitoring using Sentinel-5 (Case study: big industrial cities of Iran). Environ. Sci., 20(2), 81-98.

Fuladlu, K., & Altan, H. (2021). Examining land surface temperature and relations with the major air pollutants: A remote sensing research in case of Tehran. Urban Clim., 39, 100958.

Gharibi, S., & Shayesteh, K. (2021). Application of Sentinel 5 satellite imagery in identifying air pollutants Hotspots in Iran. J. Spat. Analysis Environ. Hazards, 8(3), 123-138.

Gheshlaghpoor, S., Abedi, S. S., & Moghbel, M. (2023). The relationship between spatial patterns of urban land uses and air pollutants in the Tehran metropolis, Iran. Landsc. Ecol., 38, 553-565.

Huang, D., He, B., Wei, L., Sun, L., Li, Y., Yan, Z., Wang, X., Chen, Y., Li, Q., & Feng, S. (2021). Impact of land cover on air pollution at different spatial scales in the vicinity of metropolitan areas. Ecol. Indic., 132, 108313.

Huang, L., Zhang, C., & Bi, J. (2017). Development of land use regression models for $PM_{2.5}$, SO_2, NO_2 and O_3 in Nanjing, China. Environ. Res., 158, 542-552.

Jacob, D. J., & Winner, D. A. (2009). Effect of climate change on air quality. Atmos. Environ., 43(1),

51-63.

Kazemi Garajeh, M., Laneve, G., Rezaei, H., Sadeghnejad, M., Mohamadzadeh, N., & Salmani, B. (2023). Monitoring trends of CO, NO_2, SO_2, and O_3 pollutants using time-series sentinel-5 images based on Google Earth Engine. Pollutants, 3(2), 255-279.

King, K. L., Johnson, S., Kheirbek, I., Lu, J. W., & Matte, T. (2014). Differences in magnitude and spatial distribution of urban forest pollution deposition rates, air pollution emissions, and ambient neighborhood air quality in New York City. Landsc. Urban Plan., 128, 14-22.

Krotkov, N. A., McLinden, C. A., Li, C., Lamsal, L. N., Celarier, E. A., Marchenko, S. V., Swartz, W. H., Bucsela, E. J., Joiner, J., & Duncan, B. N. (2016). Aura OMI observations of regional SO_2 and NO_2 pollution changes from 2005 to 2015. Atmos. Chem. Phys., 16(7), 4605-4629.

Lelieveld, J., & Dentener, F. J. (2000). What controls tropospheric ozone? Journal of Geophysical Research: Atmos., 105(D3), 3531-3551.

Lin, X., Wu, S., Chen, B., Lin, Z., Yan, Z., Chen, X., Yin, G., You, D., Wen, J., & Liu, Q. (2022). Estimating 10-m land surface albedo from Sentinel-2 satellite observations using a direct estimation approach with Google Earth Engine. ISPRS J. Photogramm. Remote Sens., 194(6375), 1-20.

Luo, J., & Gong, Y. (2023). Air pollutant prediction based on ARIMA-WOA-LSTM model. Atmos. Pollut. Res., 14(6), 101761.

McCarty, J., & Kaza, N. (2015). Urban form and air quality in the United States. Landsc. Urban Plan., 139, 168-179.

Naboureh, A., Bian, J., Lei, G., & Li, A. (2021). A Review of Land Use/Land Cover Change Mapping in the China-Central Asia-West Asia Economic Corridor Countries. Big Earth Data, 5(2), 237-257.

Nasehi, S., Nohegar, A., & Farhadi, R. (2023). Spatiotemporal analysis of urban growth patterns to provide strategies for sustainable land planning (case study: Bandar Abbas city). Geogr. Environ. Sustain., 13(4), 69-83.

Nasehi, S., Yavari, A., & Salehi, E. (2023). Investigating the spatial distribution of land surface temperature as related to air pollution level in Tehran metropolis. Pollut., 9(1), 1-14.

Nowak, D. J., Crane, D. E., & Stevens, J. C. (2006). Air pollution removal by urban trees and shrubs in the United States. Urban For Urban Green, 4(3), 115-123.

Rodríguez, M. C., Dupont-Courtade, L., & Oueslati, W. (2016). Air pollution and urban structure linkages: Evidence from European cities. Renew. Sustain. Energy Rev., 53, 1-9.

Stewart, I., & Oke, T. R. (2012). Local climate zones for urban temperature studies. Bull. Am. Meterol. Soc., 93(12), 1879-1900.

Sun, L., Chen, J., Li, Q., & Huang, D. (2020). Dramatic uneven urbanization of large cities throughout the world in recent decades. Nat. Commun., 11(1), 5366.

UNDESA. (2018). World urbanization prospects: The 2018 revision, online edition. United Nations, Department of Economic and Social Affairs (UNDESA).

Wang, Y., Guo, Z., & Han, J. (2021). The relationship between urban heat island and air pollutants and them with influencing factors in the Yangtze River Delta, China. Ecol. Indic., 129(5651), 107976.

Weng, Q., & Yang, S. (2006). Urban air pollution patterns, land use, and thermal landscape: An examination of the linkage using GIS. Environ. Monit. Assess., 117(1-3), 463-489.

Xue, R., Wang, S., Li, D., Zou, Z., Chan, K. L., Valks, P., Saiz-Lopez, A., & Zhou, B. (2020). Spatio-temporal variations in NO_2 and SO_2 over Shanghai and Chongming Eco-Island measured by Ozone Monitoring Instrument (OMI) during 2008–2017. J. Clean. Prod., 258(18), 120563.

Zabalza, J., Ogulei, D., Elustondo, D., Santamaría, J., Alastuey, A., Querol, X., & Hopke, P. (2007). Study of urban atmospheric pollution in Navarre (Northern Spain). Environ. Monit. Assess., 134(1-3), 137-151.

Zheng, S., Zhou, X., Singh, R. P., Wu, Y., Ye, Y., & Wu, C. (2017). The spatiotemporal distribution of air pollutants and their relationship with land-use patterns in Hangzhou city, China. Atmos., 8(6), 110.

Zhu, Z., Wang, G., & Dong, J. (2019). Correlation analysis between land use/cover change and air pollutants—A case study in Wuyishan city. Energies, 12(13), 2545.